



N6-methyladenosine methylation-related genes *YTHDF2*, *METTL3*, and *ZC3H13* predict the prognosis of hepatocellular carcinoma patients

Yun Wang^{1,2,3#}, Tianjun Li^{3#}, Haiping Liu⁴, Yu Liang⁴, Guanqun Wang⁵, Guangming Fu⁵, Mitsuhsa Takatsuki⁶, Haijun Qu¹, Fanbo Jing¹, Jing Li¹, Man Jiang^{1,3}

¹Department of Pharmacy, The Affiliated Hospital of Qingdao University, Qingdao University, Qingdao, China; ²Department of Radiotherapy, Qilu Hospital (Qingdao), Cheeloo College of Medicine, Shandong University, Qingdao, China; ³Precision Medicine Center of Oncology, The Affiliated Hospital of Qingdao University, Qingdao University, Qingdao, China; ⁴Department of Gastroenterology, Qingdao Municipal Hospital, Qingdao, China; ⁵Department of Pathology, The Affiliated Hospital of Qingdao University, Qingdao University, Qingdao, China; ⁶Department of Digestive and General Surgery, Graduate School of Medicine, University of the Ryukyus, Okinawa, Japan

Contributions: (I) Conception and design: M Jiang; (II) Administrative support: J Li, F Jing; (III) Provision of study materials or patients: T Li, H Qu; (IV) Collection and assembly of data: Y Wang, H Liu; (V) Data analysis and interpretation: G Wang, G Fu; (VI) Manuscript writing: All authors; (VII) Final approval of manuscript: All authors.

[#]These authors contributed equally to this work.

Correspondence to: Man Jiang. Department of Pharmacy, The Affiliated Hospital of Qingdao University, Qingdao University, Qingdao, China; Precision Medicine Center of Oncology, The Affiliated Hospital of Qingdao University, Qingdao University, Qingdao 266003, China. Email: jasmanouc@163.com.

Background: Hepatocellular carcinoma (HCC) is a common primary malignant tumor and cause of cancer-related death in humans. Increasing evidence indicates that an imbalance in N6-methyladenosine (m6A) methylation is strongly linked to the occurrence and development of cancer. We used comprehensive bioinformatics to establish a potential prognostic model of HCC based on m6A methylation-related genes. And case analyses were used to verify the results.

Methods: The clinical data and gene expressions were obtained from The Cancer Genome Atlas (TCGA) and International Cancer Genome Consortium (ICGC) databases. The prognostic value of m6A methylation-related genes in HCC patients and their relationship with the immune microenvironment were explored by comprehensive bioinformatics analyses. We also collected pathological specimens from 70 patients with HCC from the Department of Pathology, Affiliated Hospital of Qingdao University, and performed immunohistochemical staining on the specimens. We compared tumor specimens from 27 patients positive for *METTL3*, *YTHDF2*, and *ZC3H13* staining with their adjacent normal tissues and against 27 patient specimens negative for *METTL3*, *YTHDF2*, and *ZC3H13*. The influence of *METTL3*, *YTHDF2*, and *ZC3H13* on survival was analyzed, and the prognostic model for *METTL3*, *YTHDF2*, and *ZC3H13* in HCC was verified by clinical data.

Results: Most m6A methylation-related genes showed significantly different expressions between cancer and normal tissues. Three candidate m6A methylation-related genes (*YTHDF2*, *METTL3*, and *ZC3H13*) were significantly correlated with the overall survival (OS) of HCC patients. A Kaplan-Meier survival analysis indicated a worse prognosis of high-risk patients than that of low-risk patients. Immunological analysis showed that the high-risk group was more likely to have higher follicular helper T cell counts and lower resting memory CD4 T cell counts. The expression of *YTHDF2*, *METTL3*, and *ZC3H13* was validated by other databases, including the Oncomine database, the Human Protein Atlas (HPA), and the Kaplan-Meier plotter.

Conclusions: Our prognostic model based on m6A methylation-related genes effectively predicted the prognosis of HCC patients.

Keywords: Hepatocellular carcinoma (HCC); prognostic model; N6-methyladenosine methylation-related genes (m6A methylation-related genes); The Cancer Genome Atlas database (TCGA database); International Cancer Genome Consortium database (ICGC database)

Submitted Oct 20, 2022. Accepted for publication Dec 20, 2022.

doi: 10.21037/atm-22-5964

View this article at: <https://dx.doi.org/10.21037/atm-22-5964>

Introduction

Hepatocellular carcinoma (HCC) is one of the most common cancers in Asia and a common cause of cancer-related death in humans (1). It is estimated that in 2018, there were approximately 42,220 new cases of liver and intrahepatic bile duct cancers and 30,200 deaths in America (2). Moreover, the overall 1- and 3-year survival rates of HCC patients are only 36% and 17%, respectively (3). Although significant progress has been made in HCC therapy in recent years, such as surgical resection, systemic therapy, radiofrequency ablation, and liver transplantation, HCC patients' prognoses remain poor (4). Also, due to individual differences, HCC patients with the same tumor stage or other similarities in clinicopathological characteristics may have different prognoses. Hence, developing new biomarkers to precisely predict the prognosis of HCC patients is vital because HCC is a heterogeneous disease with a dismal prognosis. With

the rapid development of gene sequencing technology, multivariable prediction models have been suggested for potential biomarkers associated with HCC progression. However, the study of these multiple biomarker models is limited (5).

N6-methyladenosine (m6A) methylation is the most common RNA modification in human cells (5). Extensive research has shown that m6A methylation regulates cellular processes, including cell self-renewal, differentiation, invasion, and apoptosis, by modulating gene expression (5). Modulators of m6A methylation play a significant and pleiotropic role in the regulation of HCC. But now the studies about prognostic function of m6A genes on HCC were explored only based on bioinformatics analysis (6,7). The accurate role of m6A methylation in the tumorigenesis and progress of HCC is still not well defined neither verified by clinical cases. Messenger RNA (mRNA) and non-coding RNA (ncRNA) are involved in m6A-mediated biological processes in HCC (7). Some studies found that the most common m6A-driven regulatory functions in HCC are mRNA stability and degradation (6,7). Moreover, ncRNAs can be regulated by the m6A modification in various ways, including preprocessing, splicing, decay, and stability; thus, ncRNAs affect and participate in the m6A process of HCC (7). According to existing literature, m6A modification regulators include "writers", which are methyltransferases that are mainly responsible for transferring the methyl group to the N6 position; "readers", which are RNA-binding proteins that regulate RNA functions by recognizing specific m6A-modified positions; and "erasers", which are demethylases that remove the methyl group (8,9). The m6A methylation-related genes, including "writer" genes (*RBM15/15B*, *METTL3*, *METTL14*, *WTAP*, *VIRMA*, and *ZC3H13*), "reader" genes (*IGF2BP1/2/3*, *YTHDC1/2*, *YTHDF1/2/3*, *HNRNP*, and *eIF3*), and "eraser" genes (*ALKBH3*, *ALKBH5*, and *FTO*), interact to ensure that the dynamic and reversible balance of m6A methylation is cooperatively maintained (10).

Upon consulting the literature, we found some previous m6A methylation research in HCC. For example, *METTL3*

Highlight box

Key findings

- The m6A methylation-related genes could potential be high-risk independent prognostic factors, including *YTHDF2*, *METTL3*, and *ZC3H13*, providing a theoretical basis for the prognosis evaluation of patients with HCC.

What is known and what is new?

- High expression of *YTHDF2*, *METTL3*, *ZC3H13* was associated with higher follicular helper T cell counts and lower resting memory CD4 T cell counts, which provided our research on immune cells in the tumor microenvironment of HCC.
- High expression of *ZC3H13* is associated with poor prognosis of HCC, while high expression in clinical samples means longer survival, which provides a real-world basis for our study.

What is the implication, and what should change now?

- Multivariable prediction models of potential biomarkers associated with HCC progression could further guide the precise treatment.
- The genes of *YTHDF2*, *METTL3*, *ZC3H13* could be as the novel targets for HCC therapy.

has been found to be related to the poor prognosis of HCC patients (11). It promotes the proliferation, migration, and colony formation of HCC cells via posttranscriptional silencing of *SOCS2*, which depends on *YTHDF2* (11). In addition, *METTL14* is a reader that plays a beneficial role in HCC by regulating m6A-dependent miRNA processing (12). MiR-145 downregulates *YTHDF2* by targeting the 3'-untranslated region (3'-UTR). In summary, the upregulation of *METTL3* or downregulation of *METTL14* can predict poor prognosis for HCC patients and lead to HCC progression and metastasis (12). *METTL3* inhibits the expression of *SOCS2* in HCC via the miR-145/m6A/*YTHDF2* axis (11). These studies provide a new dimension for investigating epigenetic changes in liver cancer. To explore the prognostic model of effectively predicted the prognosis of HCC patients based on m6A methylation-related genes, in this study, we conducted extensive analyses based on The Cancer Genome Atlas (TCGA) and International Cancer Genome Consortium (ICGC) databases. We used consensus clustering analysis, least absolute shrinkage and selection operator (LASSO) regression, and Cox regression analyses to develop m6A methylation-related gene signatures. Finally, using comprehensive bioinformatics analyses, we developed a novel prognostic model based on m6A modifications as an independent risk factor predicting HCC prognosis, which we preliminarily verified with clinical cases to provide potential therapeutic targets for HCC. We present the following article in accordance with the TRIPOD reporting checklist (available at <https://atm.amegroups.com/article/view/10.21037/atm-22-5964/rc>).

Methods

Data download and processing

The potential m6A methylation-related genes, including *KIAA1429*, *METTL14*, *RBM15*, *METTL3*, *WTAP*, *ZC3H13*, *HNRNPC*, *YTHDC1*, *YTHDC2*, *YTHDF1*, *YTHDF2*, *ALKBH5*, and *FTO* were obtained. The HCC RNA-seq transcriptome and clinical data were obtained from the TCGA database. Patients with incomplete survival time, survival status, or clinicopathological characteristics were excluded. The ICGC cohort was used to validate the prognostic model.

Consensus clustering analysis

The HCC patients were clustered into different subgroups by consensus expression of m6A methylation-related genes

with the “Consensus Cluster Plus” R package (13). The accuracy of the clustering results was verified by principal component analysis (PCA). A Kaplan–Meier analysis was used to calculate the overall survival (OS) difference between clusters. The Wilcoxon rank-sum test or the Kruskal–Wallis test was used to analyze the differences in baseline characteristics, such as age, gender, grade, and stage between clusters.

Construction and validation of the prognostic model

We used a univariate Cox regression analysis to identify the prognostic m6A methylation-related genes. We performed a LASSO regression analysis, a machine learning algorithm, to eliminate over-fitting (14). All the m6A methylation-related genes identified as independent prognostic factors of OS were then screened by multivariate Cox regression analysis, and their regression coefficients were calculated.

Risk scores were conducted by multivariable fractional polynomials (MFPs) (14). The calculation was conducted as follows: $\text{risk score} = \sum_{i=1}^n v_i \times c_i$ (where v_i is the gene expression and c_i is the regression coefficient). Based on the median risk score, HCC patients were divided into high- and low-risk groups. A Kaplan–Meier survival curve was used to compare OS between the two risk subgroups. In addition, the prognostic model's accuracy was analyzed by a receiver operating characteristic (ROC) curve.

To further ensure the stability of the prognostic model, we calculated the risk score of HCC patients in the ICGC cohort. A Kaplan–Meier survival curve and survival ROC curve were developed to show the predictive ability of the prognostic model in the validation cohort. In the meantime, an independent prognostic analysis was performed to predict whether the prognostic model could be used as an independent factor for HCC prognosis.

Tumor immune microenvironment evaluation

The tumor microenvironment (TME) scores and the fraction of 21 types of immune cells were obtained from CIBERSORT in R software and were used to further explore the tumor immune microenvironment differences among different subgroups of the prognostic model. A P value <0.05 was defined as statistically significant (15).

m6A methylation-related gene validation by other databases

To explore whether the expression of m6A methylation-

Table 1 Clinical data of HCC patients in the TCGA and ICGC cohorts (17)

Clinical characteristics	TCGA cohorts (n=273)	ICGC cohorts (n=260)
Total cases		
Survival status, n (%)		
Alive	186 (68.1)	214 (82.3)
Dead	87 (31.9)	46 (17.7)
Age (years), n (%)		
<65	174 (63.7)	91 (35.0)
≥65	99 (36.3)	169 (65.0)
Gender, n (%)		
Male	186 (38.1)	192 (73.8)
Female	87 (31.9)	68 (26.2)
Tumor stage, n (%)		
I + II	196 (71.8)	157 (60.4)
III + IV	77 (28.2)	103 (39.6)
Metastasis stage, n (%)		
M0	269 (98.5)	–
M1	4 (1.5)	–

HCC, hepatocellular carcinoma; TCGA, The Cancer Genome Atlas; ICGC, International Cancer Genome Consortium.

related genes was different between HCC and other liver cancers, we analyzed several databases, including Oncomine, the Human Protein Atlas (HPA), and the Kaplan-Meier plotter online tool (16). The gene and protein expressions of the m6A methylation-related genes in HCC tissues and liver tissues were obtained from the Oncomine database and the HPA. The prognostic value of m6A methylation-related genes in HCC was verified by the Kaplan-Meier plotter online tool.

Clinical sample validation

To verify the conclusions drawn by the above analysis, we collected pathological specimens from patients from the Department of Pathology, Affiliated Hospital of Qingdao University, who had undergone liver cancer surgery (the samples had previously been analyzed and diagnosed as HCC by the Department of Pathology). Specimens from 2015 to 2020 were analyzed by immunohistochemical staining. The study was approved by the Institutional Review Board of the Affiliated Hospital of Qingdao

University Ethics Committee for Clinical Investigation (No. QYFYKYLL471311920), and conducted in accordance with the Declaration of Helsinki (as revised in 2013) and good clinical practice. All patients in our study had undergone liver surgery without comprehensive systemic treatment due to complex and heterogeneous reasons. And all of them signed informed consent of this study.

Statistical analysis

All bioinformatics analysis were performed by Perl language and R software 3.6.1. Univariate and multivariate Cox regression, LASSO regression, ROC curve, and Kaplan-Meier survival analyses were performed by R software and corresponding R packages. For all comparisons, a statistically significant difference was defined as a P value <0.05.

The clinical sample size was calculated using PASS software version 15.0 to obtain a 90% confidence level and 90% study power. In the randomized cohorts, we enrolled 54 evaluable patients, 27 of whom were positive for *METTL3*, *YTHDF2*, and *ZC3H13* staining and compared their samples with the adjacent normal tissues, and 27 patients negative for *METTL3*, *YTHDF2*, and *ZC3H13*. All patients who survived approximately 6 months or longer would provide 90% power to detect a doubling of the median progression-free survival (PFS) of more than 4.0 months at a two-sided α significance level of 0.05.

The Kaplan-Meier method was used to analyze the survival analysis of PFS and OS, and the differences between groups was evaluated by the log-rank test. The hazard ratios (HRs) were calculated by Cox proportional hazards model with 95% as their corresponding confidence intervals (CIs). For all evaluations, the P value of 0.05 was used to indicate statistical significance. The SPSS 20 software (IBM Corp., Armonk, NY, USA) and Graph Pad Prism 9 (Graph Pad Software, Inc., San Diego, CA, USA) were used to analyze all the results. All experiments were replicated three times. P<0.05 was considered a statistically significant difference.

Results

Clinical data of HCC patients

A total of 273 HCC patients were included in the TCGA cohort, comprising 186 males and 87 females from 2001 to 2020. There were 260 patients in the ICGC cohort, comprising 192 males and 68 females from 2001 to 2020 (Table 1) (17).

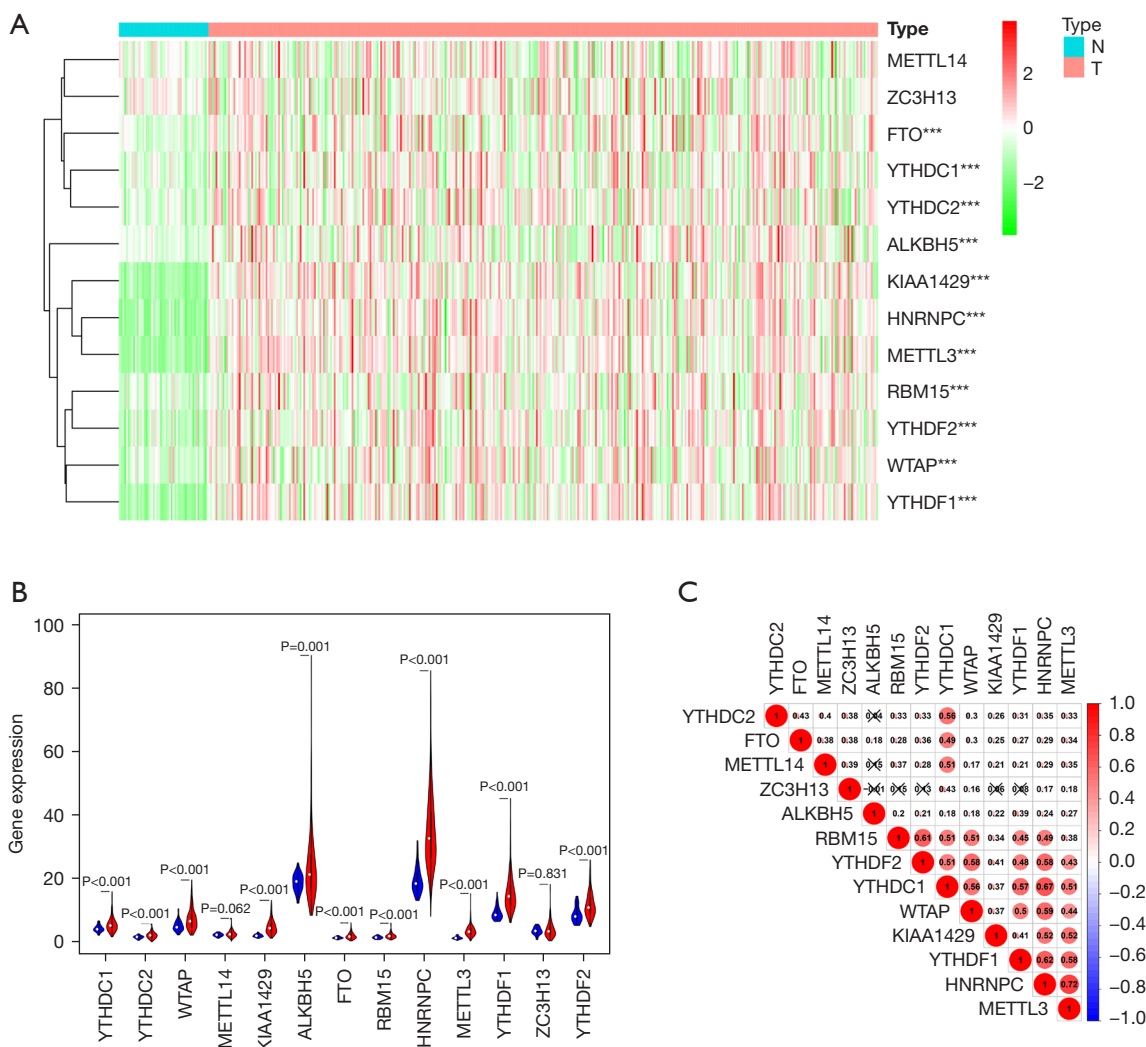


Figure 1 Figure 1 Differentially expressed m6A methylation-related genes in HCC and normal tissues. (A) The heatmap of differentially expressed m6A methylation-related genes. (B) The expression patterns of differentially expressed m6A methylation-related genes in HCC and normal tissues. Red, tumor tissues; Blue, normal tissues. (C) The correlations among m6A methylation-related genes. ***, means significant difference $P < 0.001$. N, normal tissues; T, tumor tissues; HCC, hepatocellular carcinoma; m6A, N6-methyladenosine.

Differentially expressed m6A methylation-related genes

We visualized the differential expression of m6A methylation-related genes between tumor tissues and normal tissues with a heatmap. The expression of *RBM15*, *YTHDC1*, *KIAA1429*, *YTHDC2*, *ALKBH5*, *HNRNPC*, *METTL3*, *YTHDF2*, *FTO*, *WTAP*, and *YTHDF1* was significantly higher in tumor samples than in normal tissues (Figure 1A). Additionally, the expression pattern of the differentially expressed m6A methylation-related genes was visualized by volcano plots and box plots (Figure 1B). Among all the interactions of m6A methylation-related

genes, Pearson correlation analysis showed that *METTL3* was most associated with *HNRNPC* ($r = 0.72$) (Figure 1C).

Consensus clustering of m6A methylation-related genes

To gain much more insight into the molecular heterogeneity of HCC and explore whether m6A methylation-related genes presented discernable patterns in HCC, we performed an unsupervised consensus analysis of all samples. The result of $k = 2$ seemed to be more accurate, stratifying the samples into two subgroups with less correlation between

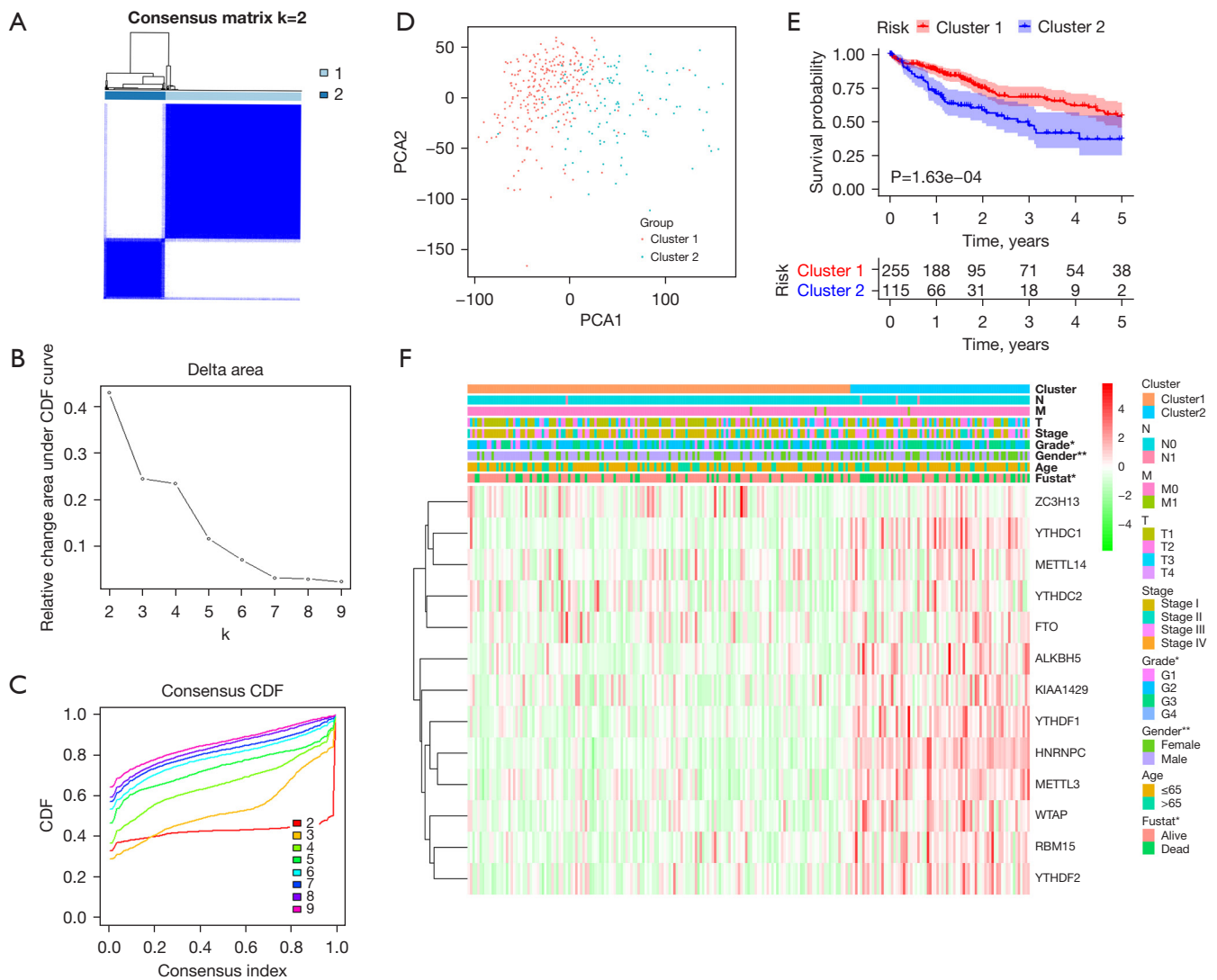


Figure 2 Tumor classification and verification based on m6A methylation-related genes. (A) The HCC patients divided into two distinct clusters, $k=2$. (B) The consensus clustering CDF for $k=2-9$. (C) The relative change in area under the CDF curve for $k=2-9$. (D) The PCA based on the m6A methylation-related genes. (E) The Kaplan-Meier survival analysis of OS in different subgroups. (F) The heatmap of m6A methylation-related gene expressions and clinicopathological features between different subgroups. *, $P<0.05$; **, $P<0.01$. PCA, principal component analysis; CDF, cumulative distribution function; N, node stage; M, metastasis stage; T, tumor stage; m6A, N6-methyladenosine; HCC, hepatocellular carcinoma; OS, overall survival.

them (Figure 2A-2C). Then, we performed a PCA to show the effect of the stratification on the transcriptional profile between cluster 1 and cluster 2 (Figure 2D). The 5-year OS of cluster 1 was significantly longer than that of cluster 2 ($P<0.001$) (Figure 2E). Then, the associations between the clusters and clinicopathological features were evaluated. Significant differences were found in features between cluster 1 and cluster 2, including grade ($P<0.05$), sex

($P<0.005$), and survival ($P<0.05$) (Figure 2F).

Construction and validation of the prognostic model

To explore the prognostic value of m6A methylation-related genes in HCC, we first performed a univariate Cox regression analysis to identify OS-associated genes (Figure 3A). Then, we performed LASSO regression and

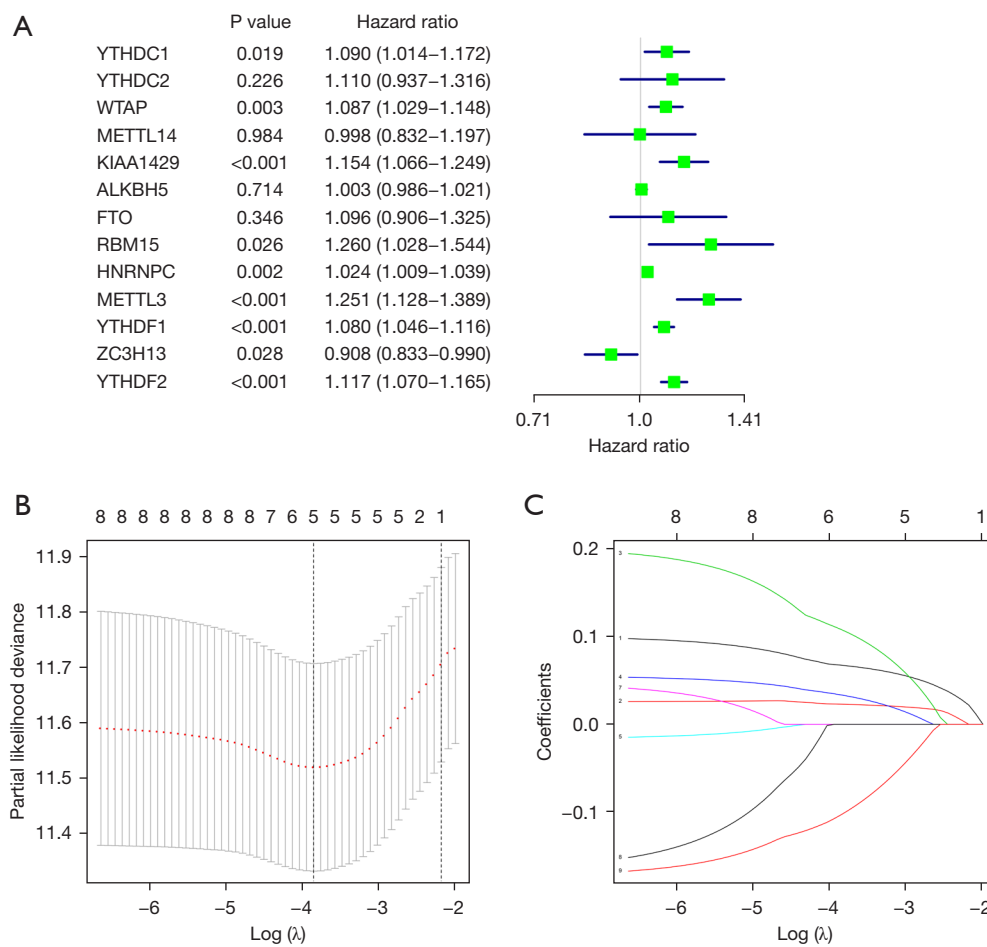


Figure 3 The univariate Cox regression and LASSO regression analyses for screening m6A methylation-related genes used in the construction of the prognostic model. (A) The univariate Cox regression analysis of m6A methylation-related genes significantly associated with survival. (B) The screening of the optimal parameter (lambda) at which the vertical lines were drawn. (C) The LASSO coefficient profiles of the five m6A methylation-related genes with non-zero coefficients determined by the optimal lambda. LASSO, least absolute shrinkage and selection operator; m6A, N6-methyladenosine.

Table 2 Three candidate m6A methylation-related genes

Gene	Coef	HR	HR.95L	HR.95H	P value
<i>YTHDF2</i>	0.094697968	1.099326773	1.050486621	1.150437645	4.42E-05
<i>METTL3</i>	0.195865822	1.216363685	1.081123362	1.368521544	0.00112586
<i>ZC3H13</i>	0.16638959	0.846716298	0.765465428	0.9365916	0.001226368

m6A, N6-methyladenosine; coef, coefficient; HR, hazard ratio; HR.95L, hazard ratio with low 95% confidence index; HR.95H, hazard ratio with high 95% confidence index.

multivariate Cox regression analyses to establish an optimal multigene prognostic model for OS, which resulted in the identification of three genes: *YTHDF2*, *METTL3*, and *ZC3H13* (Table 2, Figure 3B,3C). Our model for predicting

prognosis based on these three m6A methylation-related genes used the following formula: risk score = (*YTHDF2* expression \times 0.094698) + (*METTL3* expression \times 0.195866) + (*ZC3H13* expression \times -0.16639).

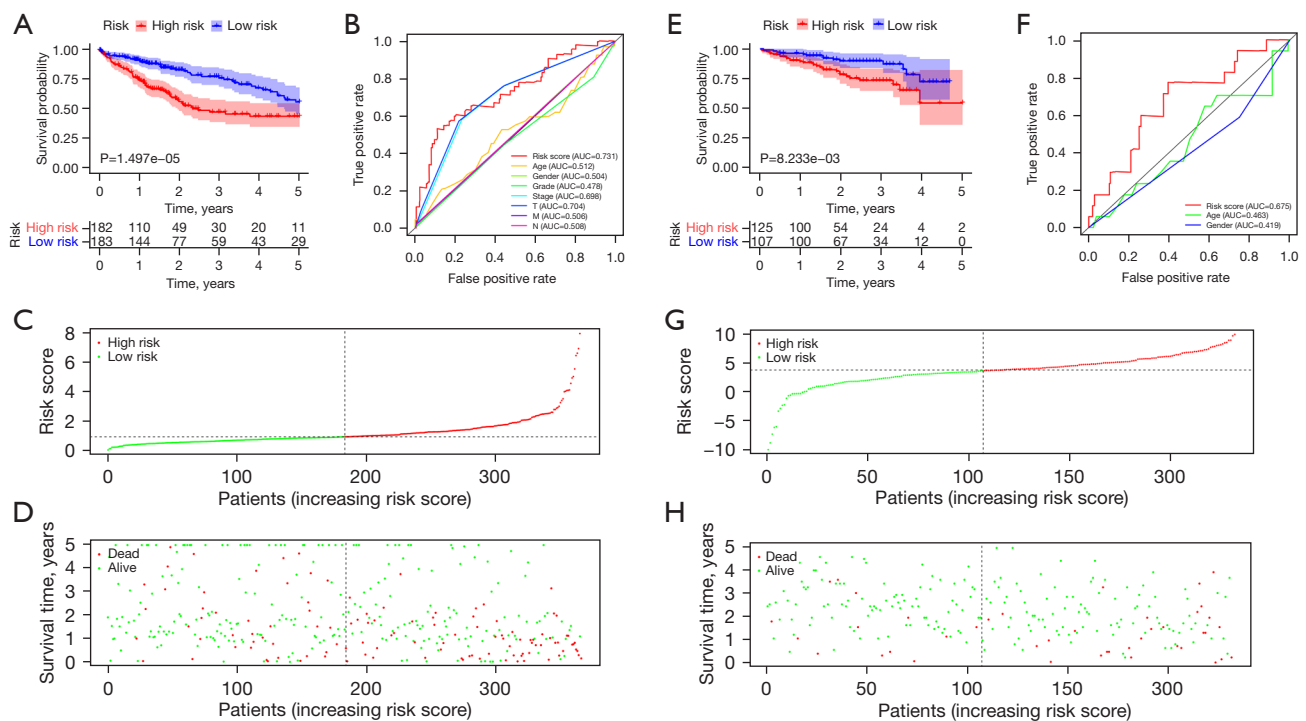


Figure 4 The prognostic model for HCC patients. (A) The Kaplan-Meier curve for the prognostic model in the TCGA cohort. (B) The ROC curve of the OS-related prognostic model in the TCGA cohort. (C) The risk score distribution of HCC patients with different risks in the TCGA cohort. (D) The scatterplots of HCC patients with different survival status in the TCGA cohort. (E) The Kaplan-Meier curve of the prognostic model in the ICGC cohort. (F) The ROC curve of the OS-related prognostic model in the ICGC cohort. (G) The risk score distribution of HCC patients with different risks in the ICGC cohort. (H) The scatterplots of HCC patients with different survival status in the ICGC cohort. AUC, area under the curve; T, tumor stage; M, metastasis stage; N, node stage; HCC, hepatocellular carcinoma; TCGA, The Cancer Genome Atlas; ROC, receiver operating characteristic; OS, overall survival; ICGC, International Cancer Genome Consortium.

HCC patients were divided into low- and high-risk groups based on the median value of the risk score. The low-risk group had a higher survival rate than the high-risk group (HR, 1.547; 95% CI, 1.320–1.812; $P < 0.001$) according to the Kaplan-Meier survival curves (Figure 4A). In addition, we assessed the accuracy of the OS-related prognostic model by constructing a ROC curve, and the AUC of the risk score was significantly higher than that of other clinicopathological parameters (Figure 4B). Finally, we ranked the HCC patients by risk score to analyze the survival distribution. As the risk score increased, the mortality rate of HCC patients also increased (Figure 4C, 4D).

We also calculated the risk score of the ICGC cohort patients (Liver Cancer-RIKEN, Japan) to validate the formula externally. Similar to the TCGA cohort, the Kaplan-Meier survival curves and the ROC curve showed that the low-risk group had a higher survival rate than the high-risk group, and the risk score had a good ability to predict

the prognosis of HCC patients ($P < 0.001$) (Figure 4E, 4F). Meanwhile, as the risk score increased, the mortality rate of HCC patients also increased (Figure 4G, 4H). Therefore, these results revealed that the prognostic signature for OS described here could effectively identify high-risk HCC patients with relatively worse OS.

The relationships between the prognostic model and immune function

According to the univariate and multivariate Cox regression analysis results ($P < 0.001$), our model can be used as a prognostic factor for HCC (Figure 5A, 5B). Thus, we evaluated the association of the prognostic model and tumor-infiltrating immune cells in the HCC immune microenvironment using the CIBERSORT algorithm. The CIBERSORT results showed that the populations of 22 types of immune cells differed between the two

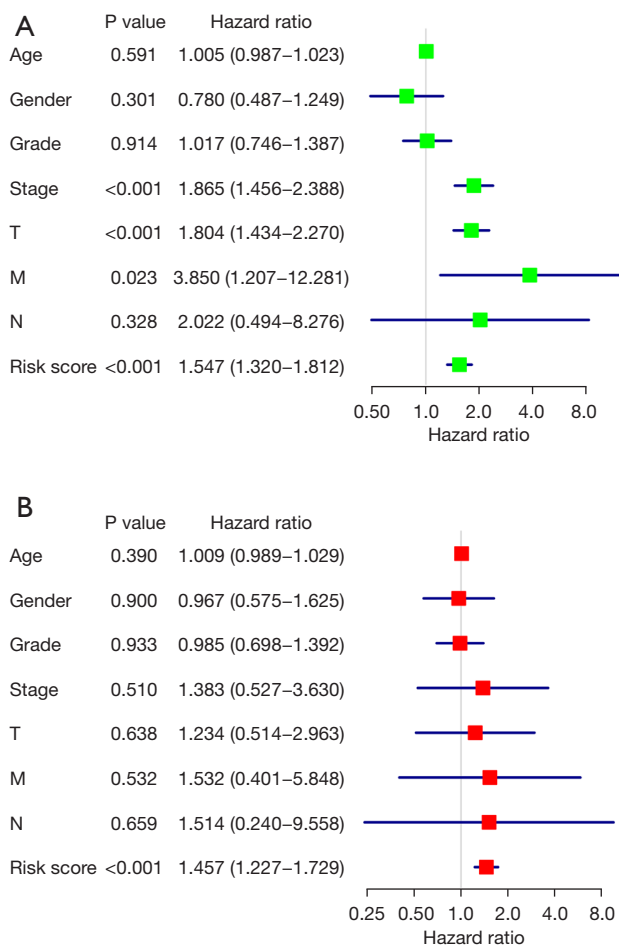


Figure 5 The independent prognostic analysis of the prognostic model. (A) Univariate factor independent prognostic analysis. (B) Multivariate factor independent prognostic analysis. T, tumor stage; M, metastasis stage; N, node stage.

subgroups (Figure 6A,6B). Moreover, there were more follicular helper T cells in the high-risk group ($P=0.016$), while there were fewer resting memory CD4 T cells in the low-risk group ($P=0.014$) (Figure 6C).

Expression of *m6A* methylation-related genes in samples from other databases

We analyzed the gene expression levels of *YTHDF2*, *METTL3*, and *ZC3H13* in samples from different databases, including the Oncomine and HPA databases and the Kaplan-Meier plotter online tool. The expression levels of *YTHDF2* and *METTL3* in HCC were higher than those in other liver cancers in two Wurmbach Liver studies (222430_

s_at, $P=0.002$; 209265_s_at, $P=1.37e-05$) (Figure 7A,7B). The expression level of *ZC3H13* showed no prognostic value in the Oncomine dataset. Moreover, we verified the histological levels of *YTHDF2*, *METTL3*, and *ZC3H13* expressions in samples from the HPA database. The results showed that the expression of *YTHDF2* and *ZC3H13* were upregulated in HCC tissues compared to normal tissues (Figure 7C,7D). The histological level of *METTL3* was not detected in samples from the HPA database. The prognostic value of *YTHDF2*, *METTL3*, and *ZC3H13* was evaluated with the Kaplan-Meier plotter online tool. We found that a high expression of *YTHDF2* (HR, 1.52; 95% CI, 1.07–2.15; log-rank $P=0.017$) and *METTL3* (HR, 1.77; 95% CI, 1.21–2.60; predicted poor survival, while a high expression of *ZC3H13* (HR, 0.43; 95% CI, 0.26–0.69; log-rank $P=0.00033$) had a higher survival (Figure 7E–7G). These results show that *YTHDF2*, *METTL3*, and *ZC3H13* are highly expressed in HCC tissues and closely related to OS in HCC patients.

Clinical sample validation

To verify the conclusions drawn by the above analysis, we collected pathological specimens from 70 patients from the Department of Pathology, Affiliated Hospital of Qingdao University who had undergone liver cancer surgery (the samples had been previously analyzed and diagnosed as HCC by the Department of Pathology), and the specimens were analyzed using immunohistochemical staining. The patients were aged 18–65, with an average age of 47. Among them, 24 were female, and 46 were male. None had hepatitis B. Among the 70 HCC specimens that underwent immunohistochemical staining, the cancer tissues were all positive for *METTL3*, *YTHDF2*, and *ZC3H13* compared with the adjacent tissues, as shown in Figure 8A–8C. Among them, in the *METTL3*-related immunohistochemical staining, 39 specimens (about 56%) were strongly stained, and 31 (about 44%) were weakly stained. In the *YTHDF2*-related immunohistochemical staining, there were 42 specimens that were strongly stained (about 60%) and 28 (about 40%) with weak staining. In the *ZC3H13*-related immunohistochemical staining, 43 specimens (about 61%) had strong staining, and 27 (about 39%) had weak staining. By collecting the clinical data of the patients, we conducted a Kaplan-Meier survival analysis. The results showed that patients with low *METTL3* expression had a longer survival time than patients with high *METTL3* expression, and patients with low *YTHDF2* expression had a longer

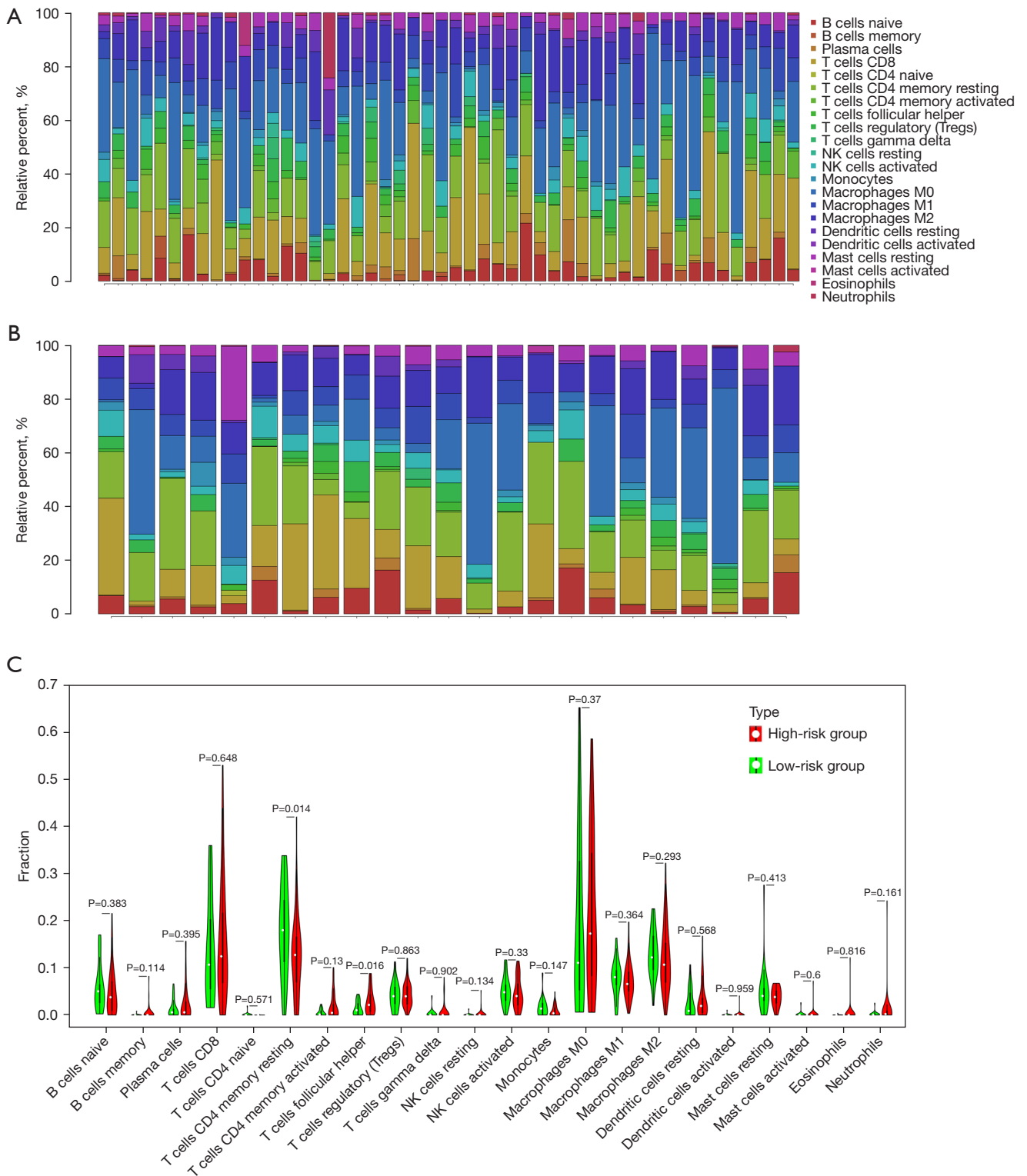


Figure 6 The comparison of the tumor immune microenvironment among different groups. (A) Twenty-two immune cells in the high-risk group. (B) Twenty-two immune cells in the low-risk group. (C) The violin plot displays the differentially expressed tumor-infiltrating immune cells in the high- and low-risk groups.

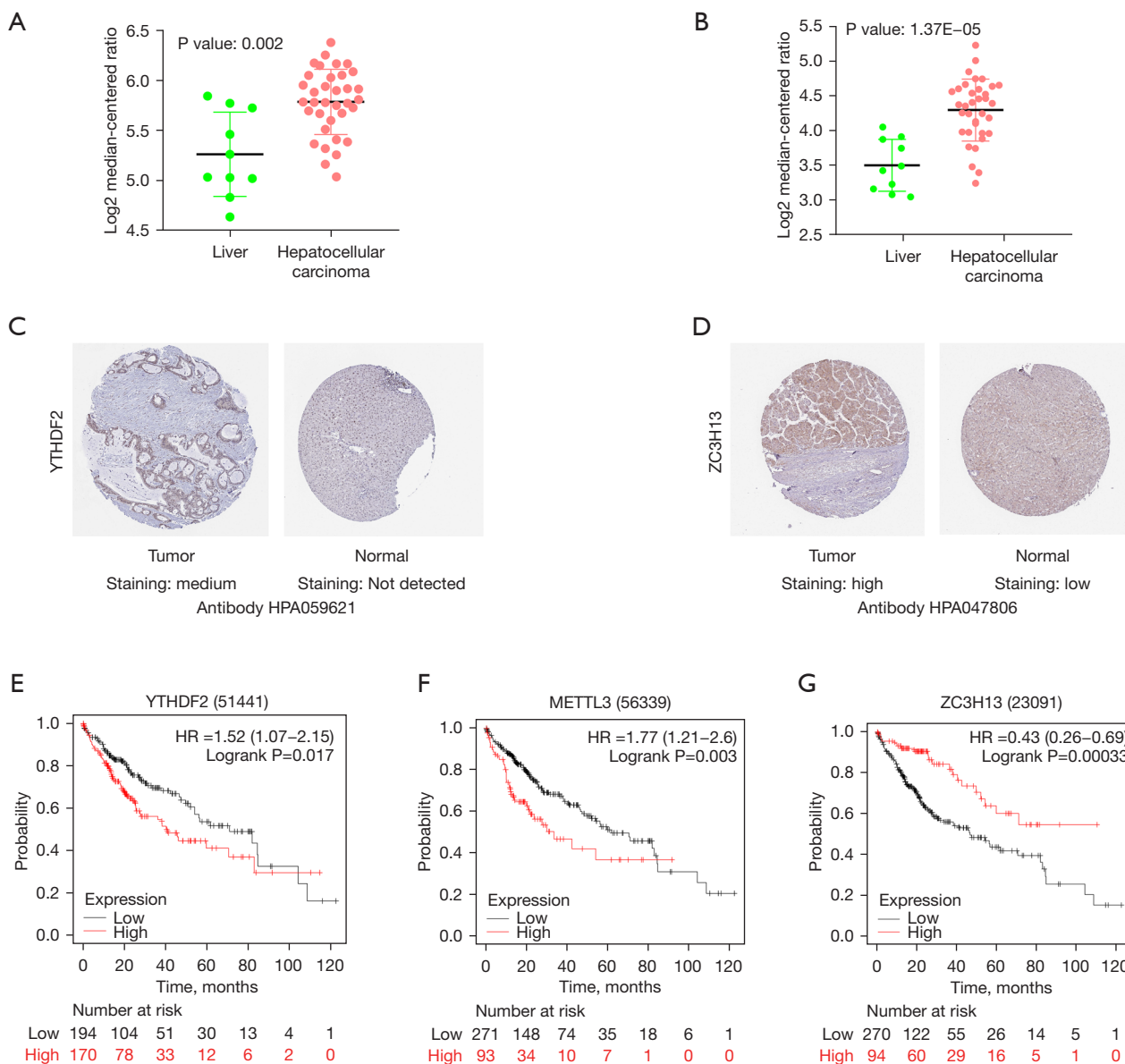


Figure 7 The expression level of *YTHDF2*, *METTL3*, and *ZC3H13* in the OncoPrint database, the HPA, and the Kaplan-Meier plotter. (A) The expression level of *YTHDF2* in HCC and other liver cancers in the OncoPrint database. (B) The expression level of *METTL3* in HCC and other liver cancers in the OncoPrint database. (C) The immunohistochemistry results of *YTHDF2* in HCC (×200) (hematoxylin-eosin staining: medium; intensity: moderate; quantity: >75%; location: nuclear) and in normal tissues (×200) (hematoxylin-eosin staining: not detected; intensity: weak; quantity: <25%; location: nuclear). (D) The immunohistochemistry results of *ZC3H13* in HCC (×200) (hematoxylin-eosin staining: medium; intensity: moderate; quantity: 75% to 25%; location: cytoplasmic/membranous) and in normal tissues (×200) (hematoxylin-eosin staining: low; intensity: weak; quantity: 75% to 25%; location: cytoplasmic/membranous nuclear). (E) The Kaplan-Meier plotter results of *YTHDF2*. (F) The Kaplan-Meier plotter results of *METTL3*. (G) The Kaplan-Meier plotter results of *ZC3H13*. HPA, Human Protein Atlas; HR, hazard ratio; HCC, hepatocellular carcinoma.

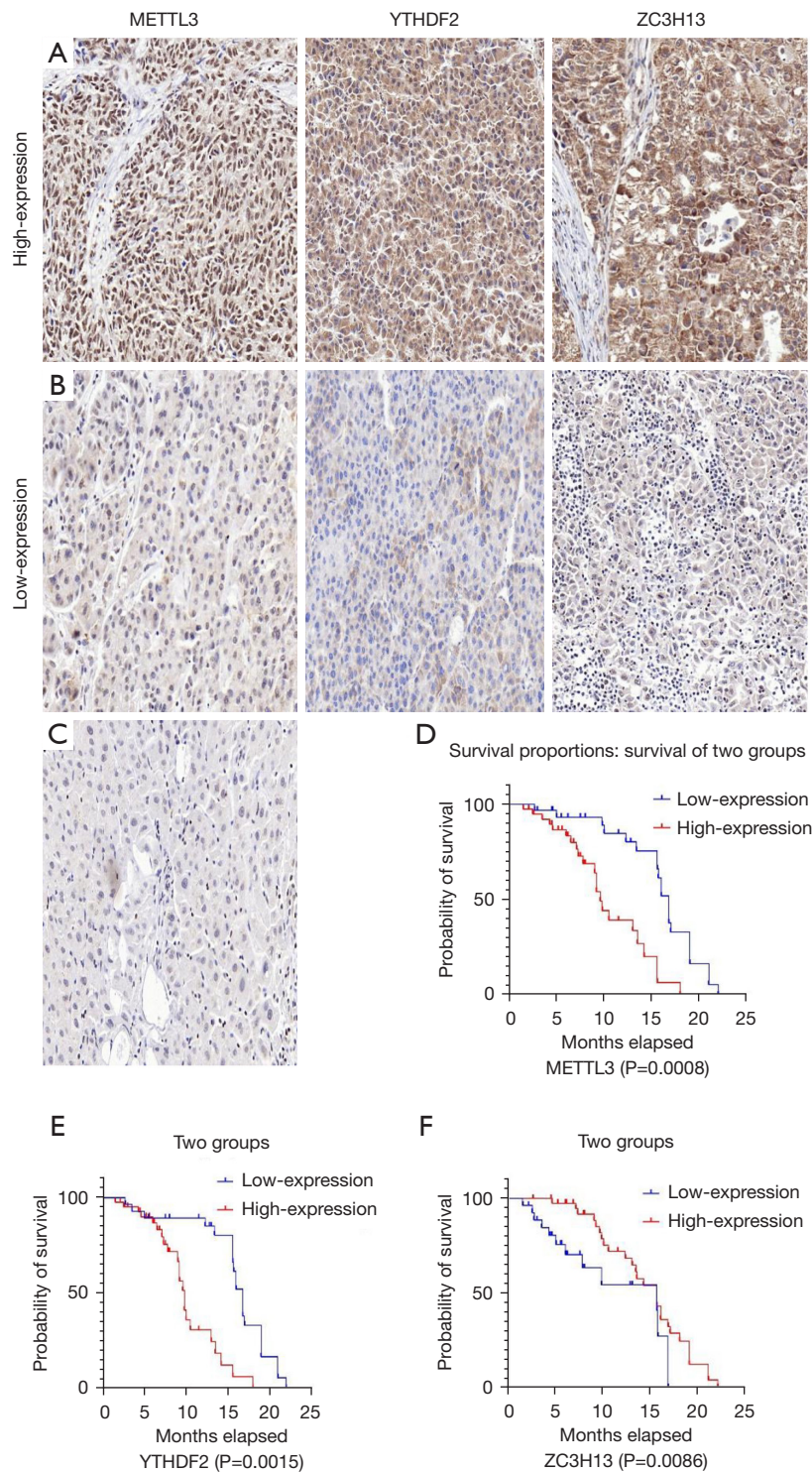


Figure 8 The analysis of *METTL3*, *YTHDF2*, and *ZC3H13* in tumor tissue. (A-C) The immunohistochemical staining contrast in paracancerous and tumor tissues ($\times 200$). (A,B) The intensity comparison of *METTL3*, *YTHDF2*, and *ZC3H13* staining in cancer tissues. (D-F) The Kaplan-Meier plotter results of *METTL3*, *YTHDF2*, and *ZC3H13*.

survival time than patients with high *YTHDF2* expression. At the same time, patients with high *ZC3H13* expression lived longer than those with low *ZC3H13* expression. This result is consistent with the above bioinformatics analysis conclusion, as shown in *Figure 8D-8F*. Further prospective study to verify the correlations between the expressions of *YTHDF2*, *METTL3*, and *ZC3H13* and the clinicopathological characteristics of HCC has been designed and added in the registered clinical trial (clinical trial No. NCT05292885).

Discussion

The HCC carcinogenesis involves an intricate regulatory network. Compared to using a single clinicopathological parameter or gene, combining diverse biomarkers and establishing a prognostic model is a more effective way to predict tumor prognosis. It is now well-established that m6A methylation plays a significant role in various types of cancer. m6A methylation is ubiquitous in the occurrence and development of cancer. A prognostic model based on selected m6A methylation-related genes may be more accurate and effective than a single clinicopathological parameter.

Herein, we analyzed the relationship between m6A methylation-related genes and the prognosis of HCC patients. We obtained the expression patterns of m6A methylation-related genes in samples from the TCGA database. Moreover, we identified three m6A methylation-related genes (*YTHDF2*, *METTL3*, *ZC3H13*) by multivariate Cox regression analysis and used them to construct the prognostic model. We verified the prognostic model via the ICGC cohort, thus indicating that the model could be used as an independent prognostic biomarker for HCC patients.

Previous studies indicated m6A genes could regulate the PD-L1 expression and immune infiltration in multiple solid tumors (18-20). But in HCC the relationship between m6A regulation and tumor immune microenvironment remains ambiguous. A study of 18 m6A regulators (21) indicated HCC patients with higher m6A scores associated with higher PD-L1 expression. However, the patient with low m6A scores might be benefit from immune checkpoint inhibitor therapy according to clinical outcomes. May be the m6A regulation group of the study mentioned above both associated the PD-L1 expression and TME cell infiltration (21). Although the results was still debated, it can be confirmed that m6A

regulation is a potential biomarker for prognostic prediction of immunotherapy for HCC. And the accurate prognostic model should further explored. Herein, the CIBERSORT results showed higher counts of follicular helper T cells in the high-risk group, while the resting memory CD4 T cell counts were higher in the low-risk group. Follicular helper T cells, which are key regulators in the tumor immune microenvironment, are a specialized type of T cell that helps B cells and drives the response of germinal centers (22-24). Recent evidence suggests that follicular helper T cells participate in antitumor immune responses (25). However, only a few studies have reported the relationship between resting CD4 memory T cells and cancer immunotherapy. According to these results high-risk patients identified by our prognostic model may be sensitive to immunotherapy. And our results indicated a novel insight to the relationship of the m6A regulation and the HCC immunotherapy.

YTHDF2, the first functionally verified m6A reader, promotes the degradation of m6A-modified mRNAs in humans (26). A previous study has shown that *YTHDF2* destabilizes m6A-containing RNA via direct recruitment of the CCR4-NOT deadenylase complex. And the CCR4-NOT deadenylase complex is recruited to m6A-containing RNAs through a direct interaction with the N-terminal region of *YTHDF2* (27). *YTHDF2* has a vast impact on mRNA degradation in different tissues and cell types in vertebrates (28). In addition, *YTHDF2* may act as a tumor suppressor to repress cell proliferation and growth by destabilizing *EGFR* mRNA in HCC cells (29). Our results further revealed that *YTHDF2* might play an important role in liver cancer development and could be used as a therapeutic target for HCC patients. *METTL3*, a RNA methyltransferase, has been implicated in mRNA decay, biogenesis, and translation control through m6A modification (30). Some studies have shown that *METTL3*-mediated m6A modification is involved in regulating numerous genes in various types of cancer (30-33). Moreover, one study reported that crosstalk between *METTL3* and miR-186 regulates hepatoblastoma progression through the Wnt/ β -catenin signaling pathway (34). Another study showed that *METTL3* promotes the progression of HCC via m6A-mediated upregulation of microRNA-873-5p (35). Our observations suggest that *METTL3* abnormalities contribute to an increased risk of developing HCC. *ZC3H13*, a canonical CCCH zinc finger protein, plays an important role in modulating RNA m6A methylation in the nucleus (36,37). One report has stated that *ZC3H13* suppresses colorectal

cancer proliferation and invasion by inactivating Ras-ERK signaling (36). However, there are few studies about the mechanism of *ZC3H13* in cancer. Our findings suggest that *ZC3H13* is a promising diagnostic marker in HCC. The HCC RNA-seq transcriptome and clinical data in our study were all obtained from the TCGA database. All the conclusion should be verified and other biomarkers should be further studied by clinical trials. According to our study, the *YTHDF2*, *METTL3*, and *ZC3H13* potential predict the prognosis of HCC patients independently. And the interactions of the three genes should be further explored.

In addition, we assessed the expression of the three m6A methylation-related genes in samples from other databases. *YTHDF2*, *METTL3*, and *ZC3H13* were highly expressed in HCC tissues and closely related to OS in HCC patients. Based on existing reports, the mechanism of *YTHDF2*, *METTL3*, and *ZC3H13* in HCC remains unclear. Our study firstly used multiple databases to establish a prognostic model related to *YTHDF2*, *METTL3*, and *ZC3H13* expression for the prognosis predicting of HCC, which maybe provide novel treatment strategy for HCC. However, our research still has certain limitations. Firstly, it is a retrospective study, there may be biases concerning the choice of variables. Second, the mechanisms of action of the m6A methylation-related genes in HCC need to be validated by *in vivo* and *in vitro* experiments to confirm our results. Third, all the samples were nonrepresentative, and samples from clinical trials should be further studied. Finally, our sample size was limited with few events per predictor. And missing data may have also potentially influenced the objectivity of the study.

Conclusions

In conclusion, our research systematically demonstrated that the m6A methylation-related genes *YTHDF2*, *METTL3*, and *ZC3H13* were significantly associated with the tumor microenvironment and may have further potential to effectively predict the prognosis of HCC patients.

Acknowledgments

The authors appreciate the academic support from the AME Hepatocellular Carcinoma Collaborative Group.

Funding: This study was supported, in part, by Shandong Medical and Health Science and Technology Development Program (No. 202102040497).

Footnote

Reporting Checklist: The authors have completed the TRIPOD reporting checklist. Available at <https://atm.amegroups.com/article/view/10.21037/atm-22-5964/rc>

Data Sharing Statement: Available at <https://atm.amegroups.com/article/view/10.21037/atm-22-5964/dss>

Conflicts of Interest: All authors have completed the ICMJE uniform disclosure form (available at <https://atm.amegroups.com/article/view/10.21037/atm-22-5964/coif>). The authors have no conflicts of interest to declare.

Ethical Statement: The authors are accountable for all aspects of the work in ensuring that questions related to the accuracy or integrity of any part of the work are appropriately investigated and resolved. The study was approved the Institutional Review Board of the Affiliated Hospital of Qingdao University Ethics Committee for Clinical Investigation (No. QYFYKYLL471311920) and conducted in accordance with the Declaration of Helsinki (as revised in 2013) and good clinical practice. Informed consent was taken from all the patients.

Open Access Statement: This is an Open Access article distributed in accordance with the Creative Commons Attribution-NonCommercial-NoDerivs 4.0 International License (CC BY-NC-ND 4.0), which permits the non-commercial replication and distribution of the article with the strict proviso that no changes or edits are made and the original work is properly cited (including links to both the formal publication through the relevant DOI and the license). See: <https://creativecommons.org/licenses/by-nc-nd/4.0/>.

References

1. Nakano S, Eso Y, Okada H, et al. Recent Advances in Immunotherapy for Hepatocellular Carcinoma. *Cancers (Basel)* 2020;12:775.
2. Bray F, Ferlay J, Soerjomataram I, et al. Global cancer statistics 2018: GLOBOCAN estimates of incidence and mortality worldwide for 36 cancers in 185 countries. *CA Cancer J Clin* 2018;68:394-424.
3. El-Serag HB. Hepatocellular carcinoma: recent trends in the United States. *Gastroenterology* 2004;127:S27-34.
4. Zheng Z, Liang W, Wang D, et al. Adjuvant chemotherapy for patients with primary hepatocellular carcinoma: a

- meta-analysis. *Int J Cancer* 2015;136:E751-9.
5. Huo J, Wu L, Zang Y. Development and validation of a CTNNB1-associated metabolic prognostic model for hepatocellular carcinoma. *J Cell Mol Med* 2021;25:1151-65.
 6. Huang H, Bai Y, Lu X, et al. N6-methyladenosine associated prognostic model in hepatocellular carcinoma. *Ann Transl Med* 2020;8:633.
 7. Lu J, Qian J, Yin S, et al. Mechanisms of RNA N(6)-Methyladenosine in Hepatocellular Carcinoma: From the Perspectives of Etiology. *Front Oncol* 2020;10:1105.
 8. Liu N, Dai Q, Zheng G, et al. N(6)-methyladenosine-dependent RNA structural switches regulate RNA-protein interactions. *Nature* 2015;518:560-4.
 9. Meyer KD, Jaffrey SR. Rethinking m(6)A Readers, Writers, and Erasers. *Annu Rev Cell Dev Biol* 2017;33:319-42.
 10. Wang T, Kong S, Tao M, et al. The potential role of RNA N6-methyladenosine in Cancer progression. *Mol Cancer* 2020;19:88.
 11. Chen M, Wei L, Law CT, et al. RNA N6-methyladenosine methyltransferase-like 3 promotes liver cancer progression through YTHDF2-dependent posttranscriptional silencing of SOCS2. *Hepatology* 2018;67:2254-70.
 12. Ma JZ, Yang F, Zhou CC, et al. METTL14 suppresses the metastatic potential of HCC by modulating m6A-dependent primary miRNA processing. *Hepatology* 2017;65:529-43.
 13. Wilkerson MD, Hayes DN. ConsensusClusterPlus: a class discovery tool with confidence assessments and item tracking. *Bioinformatics* 2010;26:1572-3.
 14. Sauerbrei W, Royston P, Binder H. Selection of important variables and determination of functional form for continuous predictors in multivariable model building. *Stat Med* 2007;26:5512-28.
 15. Chen B, Khodadoust MS, Liu CL, et al. Profiling Tumor Infiltrating Immune Cells with CIBERSORT. *Methods Mol Biol* 2018;1711:243-59.
 16. Wang L, Zhou N, Qu J, et al. Identification of an RNA binding protein-related gene signature in hepatocellular carcinoma patients. *Mol Med* 2020;26:125.
 17. Rhodes DR, Yu J, Shanker K, et al. ONCOMINE: a cancer microarray database and integrated data-mining platform. *Neoplasia* 2004;6:1-6.
 18. Yi L, Wu G, Guo L, et al. Comprehensive Analysis of the PD-L1 and Immune Infiltrates of m6A RNA Methylation Regulators in Head and Neck Squamous Cell Carcinoma. *Mol Ther Nucleic Acids* 2020;21:299-314.
 19. Zhang B, Wu Q, Li B, et al. m(6)A regulator-mediated methylation modification patterns and tumor microenvironment infiltration characterization in gastric cancer. *Mol Cancer*. 2020;19:53
 20. Chong W, Shang L, Liu J, et al. m6A regulator-based methylation modification patterns characterized by distinct tumor microenvironment immune profiles in colon cancer. *Theranostics* 2021;11:2201-17.
 21. Yin T, Zhao L, Yao S. Comprehensive characterization of m6A methylation and its impact on prognosis, genome instability, and tumor microenvironment in hepatocellular carcinoma. *BMC Med Genomics* 2022;15:53.
 22. Hetta HF, Elkady A, Yahia R, et al. T follicular helper and T follicular regulatory cells in colorectal cancer: A complex interplay. *J Immunol Methods* 2020;480:112753.
 23. Guisier F, Barros-Filho MC, Rock LD, et al. Janus or Hydra: The Many Faces of T Helper Cells in the Human Tumour Microenvironment. *Adv Exp Med Biol* 2020;1224:35-51.
 24. Panneton V, Chang J, Witalis M, et al. Inducible T-cell co-stimulator: Signaling mechanisms in T follicular helper cells and beyond. *Immunol Rev* 2019;291:91-103.
 25. Qian G, Wu M, Zhao Y, et al. Thyroid cancer metastasis is associated with an overabundance of defective follicular helper T cells. *APMIS* 2020;128:487-96.
 26. Wang X, Lu Z, Gomez A, et al. N6-methyladenosine-dependent regulation of messenger RNA stability. *Nature* 2014;505:117-20.
 27. Du H, Zhao Y, He J, et al. YTHDF2 destabilizes m(6)A-containing RNA through direct recruitment of the CCR4-NOT deadenylase complex. *Nat Commun* 2016;7:12626.
 28. Fei Q, Zou Z, Roundtree IA, et al. YTHDF2 promotes mitotic entry and is regulated by cell cycle mediators. *PLoS Biol* 2020;18:e3000664.
 29. Zhong L, Liao D, Zhang M, et al. YTHDF2 suppresses cell proliferation and growth via destabilizing the EGFR mRNA in hepatocellular carcinoma. *Cancer Lett* 2019;442:252-61.
 30. Lin S, Choe J, Du P, et al. The m(6)A Methyltransferase METTL3 Promotes Translation in Human Cancer Cells. *Mol Cell* 2016;62:335-45.
 31. Cai X, Wang X, Cao C, et al. HBXIP-elevated methyltransferase METTL3 promotes the progression of breast cancer via inhibiting tumor suppressor let-7g. *Cancer Lett* 2018;415:11-9.
 32. Lin A, Zhou M, Hua RX, et al. METTL3 polymorphisms and Wilms tumor susceptibility in Chinese children: A

- five-center case-control study. *J Gene Med* 2020;22:e3255.
33. Liu ZF, Yang J, Wei SP, et al. Upregulated METTL3 in nasopharyngeal carcinoma enhances the motility of cancer cells. *Kaohsiung J Med Sci* 2020;36:895-903.
 34. Cui X, Wang Z, Li J, et al. Cross talk between RNA N6-methyladenosine methyltransferase-like 3 and miR-186 regulates hepatoblastoma progression through Wnt/ β -catenin signalling pathway. *Cell Prolif* 2020;53:e12768.
 35. Zhao M, Jia M, Xiang Y, et al. METTL3 promotes the progression of hepatocellular carcinoma through m6A-mediated upregulation of microRNA-873-5p. *Am J Physiol Gastrointest Liver Physiol* 2020;319:G636.
 36. Zhu D, Zhou J, Zhao J, et al. ZC3H13 suppresses colorectal cancer proliferation and invasion via inactivating Ras-ERK signaling. *J Cell Physiol* 2019;234:8899-907.
 37. Wen J, Lv R, Ma H, et al. Zc3h13 Regulates Nuclear RNA m(6)A Methylation and Mouse Embryonic Stem Cell Self-Renewal. *Mol Cell* 2018;69:1028-38.e6.
- (English Language Editor: D. Fitzgerald)

Cite this article as: Wang Y, Li T, Liu H, Liang Y, Wang G, Fu G, Takatsuki M, Qu H, Jing F, Li J, Jiang M. N6-methyladenosine methylation-related genes YTHDF2, METTL3, and ZC3H13 predict the prognosis of hepatocellular carcinoma patients. *Ann Transl Med* 2022;10(24):1398. doi: 10.21037/atm-22-5964